coatings

MDPI

Article

Effect of Vacancy Defects and Hydroxyl on the Adsorption of Glycine on Mg(0001): A First-Principles Study

Zhe Fang [1,2], Wutao Wei [1,*], Huijie Qiao [1], Erjun Liang [2,*], Yu Jia [2,3] and Shaokang Guan [4]

[1] School of Materials and Chemical Engineering, Center for Advanced Materials Research, Zhongyuan University of Technology, Zhengzhou 450007, China
[2] International Laboratory for Quantum Functional Materials of Henan & School of Physics and Microelectronics, Zhengzhou University, Zhengzhou 450001, China
[3] Key Laboratory for Special Functional Materials of Ministry of Education, Henan University, Kaifeng 475004, China
[4] School of Materials Science and Engineering, Zhengzhou University, Zhengzhou 450001, China
* Correspondence: 9889@zut.edu.cn (W.W.); ejliang@zzu.edu.cn (E.L.)

Abstract: Glycine (Gly), as one of the fundamental components of biomolecules, plays a crucial role in functional biomolecular coatings. The presence of structural defects and hydroxyl-containing functional groups in magnesium (Mg) materials, which are commonly used as biomedical materials, significantly affects their biocompatibility and corrosion resistance performance. This study computationally investigates the influence of vacancy defects and hydroxyl groups on the adsorption behavior of Gly on Mg(0001) surfaces. All potential adsorption configurations are considered through first-principles calculations. The findings indicate that stronger chemisorption occurs when Gly is positioned at the edge of the groove, where the surface has a vacancy defect concentration of 1/3. Among the four adsorption locations, the fcc-hollow site is determined to be the most favorable adsorption site for hydroxyl. The adsorption energy of Gly on the Mg(0001) surface containing the hydroxyl (−1.11 eV) is 0.05 eV more than that of on the Mg(0001) surface (−1.16 eV). The adsorption energies, electronic properties, charge transfer, and stable configurations are calculated to evaluate the interaction mechanism between Gly and defective surfaces. Calculated results provide a comprehensive understanding of the interaction mechanism of biomolecules on defective Mg surfaces and also indicate the directions for future experimental research.

Keywords: glycine; Mg; defect; first-principles calculation; adsorption

Citation: Fang, Z.; Wei, W.; Qiao, H.; Liang, E.; Jia, Y.; Guan, S. Effect of Vacancy Defects and Hydroxyl on the Adsorption of Glycine on Mg(0001): A First-Principles Study. *Coatings* **2023**, *13*, 1684. https://doi.org/10.3390/coatings13101684

Academic Editor: Alessandro Patelli

Received: 30 August 2023
Revised: 19 September 2023
Accepted: 22 September 2023
Published: 26 September 2023

1. Introduction

The initial reactions of biological magnesium (Mg) alloy materials in the physiological environment of the human body depend on their surface properties [1–5]. Surface modification is one of the most commonly used methods to regulate the interaction between biomaterials and internal tissues, improving the biocompatibility and corrosion resistance of Mg alloys [6–12]. The optimal treatment and disease diagnosis are achieved through this method to better adapt to physiological environments and provide required clinical performance requirements.

Investigating the interaction between material surfaces with different microstructures and biomolecules has important clinical applications. It is difficult to obtain the perfect crystal surface with atoms arranged regularly and completely due to the influence of atoms (or ions and molecules), the formation conditions of crystals, cold or hot processing, and some crystal defects [13–15]. Crystal defects are mainly divided into vacancy defects, line defects, and surface defects according to the geometric characteristics, and common vacancy defects mainly include vacancy, interstitial particles, and foreign particles. Han et al. used the first-principles calculation method based on density functional theory and found that the presence of vacancy defects enhances the reaction activity of the Mg(0001)

surface and reduces the diffusion barrier of hydrogen on the surface [16]. The calculated results by Zhou et al. through the first-principles calculation indicate that the addition of transition metals on the Mg surface makes a strong interaction between the transition metals and Mg atoms, and the diffusion process of the transition metal atoms is difficult to produce due to the higher potential barrier [17].

For the study of the adsorption of hydroxyl on the surface of Mg, the results of Williams et al. reported that the adsorption of hydroxyl on the surface of Mg is relatively stable in a neutral environment with a pH value of 7. The stable adsorption of hydroxyl reduced the work function of the Mg surface, which will be beneficial for the hydrogen release process [18]. Yuwono et al. found that the stability of the Mg surface is related to the concentration of hydroxyl adsorbed. A certain concentration of hydroxyl adsorbed on the Mg surface decreases the surface work function, which is conducive to the progress of chemical reactions [19]. Zhou et al. calculated the different bromine coverage on the Mg(0001) surface and found that the adsorption is most stable at the fcc-hollow site with the bromine coverage being 0.25–1.00 ML, and the adsorption energy decreases, and the work function increases with the increase of the coverage [20]. Li et al. modified the metal surface state by doping, introducing defects, or adsorbing other radicals to prompt the hydride formation and revealed the nature of this phenomenon in the Mg corrosion via the first-principles calculation [21].

Amino acids, as the fundamental units of proteins, are interesting adsorbents for studying the interaction between biomolecules and solid surfaces [22]. These organic molecules exhibit various charges, polarities, water interactions, and proton exchanges. A common feature is that they are composed of an amino group and a carboxyl group, but there is a unique functional group in the side chain. They are the fundamental units of complex biological molecules containing peptides and proteins. Gly is one of the basic components of biological molecules and a nonessential amino acid that exists in neutral and zwitterionic forms. A single carbon molecule is linked to an amino and a carboxyl group, making it the simplest amino acid among all amino acids [23,24]. The investigation of the surface structure and properties of Gly and biomaterials is not only a significant subject in the fields of life sciences and medicine but also a crucial scientific matter in the domains of chemistry, materials science, and the pharmaceutical industry [25–30]. Kumar et al. optimized the adsorption geometries of Gly and suggested covalent bonding between N and O atoms of the molecules and the surface Cu-atoms [24]. Madden et al. [31] carried out both experimental and computational investigations to shed light on the adsorption behavior of glycine on this specific Cu(311) surface and found that Gly adsorbs onto Cu(311) with the nitrogen atom and one or two oxygen atoms of the carboxylic acid group bonding to copper atoms in an adjacent row. These simulations helped explain the specific bonding arrangements observed in the experimental results.

The adsorption and reactivity of Gly on Mg and Mg-based alloy surfaces, as well as the interaction mechanism between biomolecules and different Mg surfaces, were investigated in our previous work [32–35]. In the present work, the influence of surface vacancy defects concentration (1/36, 1/6, 1/3, and 1/2) and hydroxyl on the adsorption characteristics of Gly on the Mg(0001) surface was systematically investigated and discussed based on the density functional theory (DFT). Our theoretical studies help us propose scenarios for the adsorption mechanism of Gly/Mg(0001) and elucidate their dependence on different surface vacancy concentrations. The anticipated computational results will provide a better understanding of the reactivity of Mg-defected crystal surfaces and hydroxyl groups during the adsorption process of glycine. This understanding will facilitate the design of Mg surfaces with enhanced performance.

2. Computational Methods

All DFT calculations were performed using the Vienna Ab initio Simulation Package (VASP) with the projector-augmented wave (PAW) method to characterize the interaction between ions and valence electrons [36–38]. The exchange-correlation function was dealing

with GGA-PBE [39]. Dion et al. [40] and Klimeŝ et al. [41–43] have proposed the local van der Waals density functional scheme for the van der Waals contributions. Calculations of the present work were performed by the optB86b-vdW method [44]. The plane wave cut-off energy was set to 400 eV to describe the valance electrons. Six atomic layer thicknesses with four vacancy defect concentrations of 1/36, 1/6, 1/3, and 1/2 were chosen as the surface model, and the bottom two layers of Mg atoms were fixed throughout the optimization. The concentration of four vacancy defects is primarily distributed in the topmost atomic layer of the surface model. The bottom two layers of Mg atoms were fixed throughout the optimization with the vacuum of 20 Å, and the optimized glycine molecule was placed above the Mg(0001) surface. The ground state convergence criterion was set to 10^{-5} eV, and all atoms were allowed to fully relax until the Hellmann-Feynman forces were smaller than 0.02 eV/Å during the geometry optimization process.

The calculation of the adsorption energy (E_{ads}) of Gly on different substrates is as follows:

$$E_{ads} = E_{mol} + E_{sub} - E_{mol+sub} \quad (1)$$

where E_{mol}, E_{sub}, and $E_{mol+sub}$ represent the total energy of the optimized Gly, the energy of different substrates, and the energy of the stable adsorption systems, respectively.

3. Results and Discussion

Gly is primarily composed of an amino group and a carboxyl group, making it the simplest structure in the amino acid sequence. The interaction between amino acids and the surface mainly includes van der Waals and electrostatic interactions, and surface charges significantly affect the adsorption of amino acids [7]. The optimized structure of Gly is shown in Figure 1a, and the bond lengths of C1-N1, C2-O1, and C2-O2 are 1.45 Å, 1.21 Å, and 1.36 Å, respectively. The hexagonal close-packed crystal structure of Mg is depicted in Figure 1b, and the optimized lattice parameters of the bulk hcp Mg are a = b = 3.188 Å and c = 5.193 Å, which are in good agreement with the experimental results (a = b = 3.210 Å, c = 5.213 Å) [45] as well as the previously calculated results (a = b = 3.193 Å, c = 5.185 Å) [46]. For the adsorption of the isolated hydroxyl, four adsorption sites (bridge, top, fcc-hollow, and hcp-hollow sites) on the Mg(0001) surface are shown in Figure 1c.

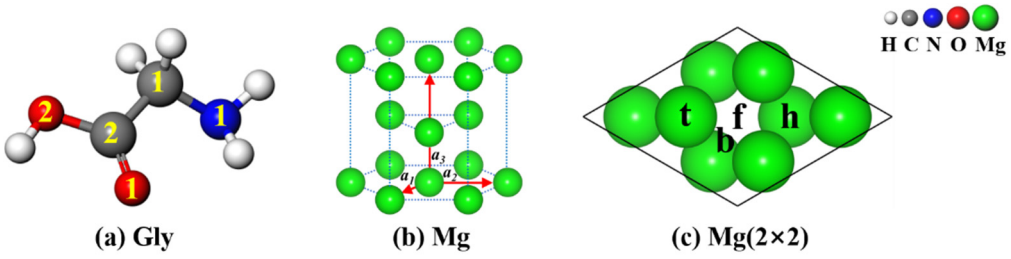

Figure 1. (**a**) Optimized structure of Gly. (**b**) The crystal structure of Mg. (**c**) Four adsorption sites (bridge, top, fcc-hollow, and hcp-hollow sites) on the surface of Mg(0001).

3.1. Adsorption of Gly on the Mg(0001) Surfaces with Different Defect Concentrations

The isolated adsorption behavior of Gly on the Mg(0001) surface was reported earlier, and the strongest interaction occurs when the amino and carboxyl groups in glycine adsorbed on the Mg(0001) surface simultaneously, according to the calculated results [32]. The electronic structural properties of the Mg surface are altered by the presence of a vacancy defect in the optimized defect-free cleaved Mg(0001) surface. In this study, the adsorption behavior of Gly on the Mg(0001) surface with four different surface vacancy defect concentrations (1/36, 1/6, 1/3, and 1/2) was investigated to establish a correlation between the electronic properties of Gly and the surfaces. The optimized surfaces of four energetically significant configurations with varying vacancy defect concentrations (1/36, 1/6, 1/3, and 1/2) are illustrated in Figure 2.

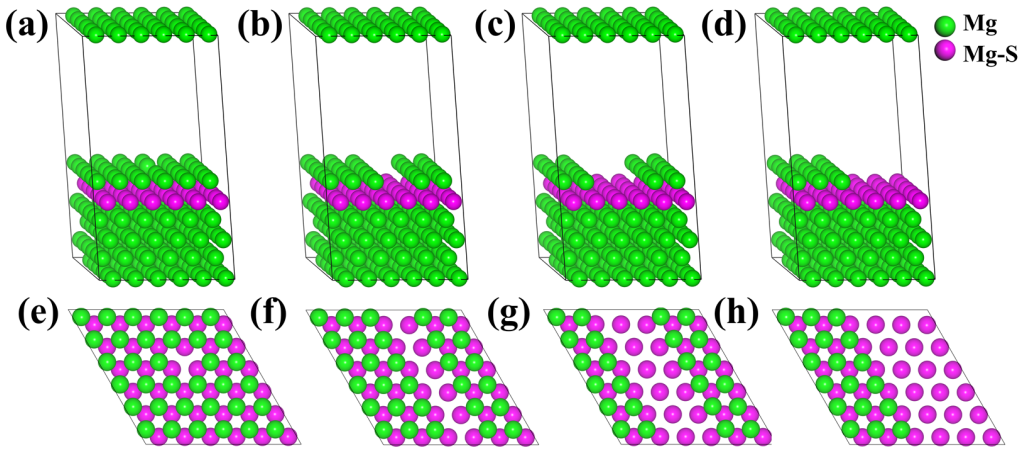

Figure 2. (**a**–**d**) provide side views, and (**e**–**h**) show top views of four different Mg(0001) surfaces with varying vacancy defect concentrations of (**a**) 1/36, (**b**) 1/6, (**c**) 1/3, and (**d**) 1/2. The Mg-S notation indicates the Mg atoms in the second layer.

As reported in Ref. [32] regarding the adsorption of Gly on the Mg(0001) surface, it is important to note that the N atom in the amino group and the O atom in the carboxyl group primarily interact with the surface Mg atoms. The coordination covalent bonds formed between N-Mg and O-Mg contribute to stronger interactions. To investigate the adsorption behavior of Gly on surfaces with vacancy defects, the adsorption energies of Gly on the Mg surface were calculated at the four different vacancy defect concentrations mentioned above. The adsorption energies of Gly on the Mg surface after reaching a stable adsorption state are listed in Table 1, and the adsorption configurations of Gly on the Mg(0001) surface are depicted in Figure 3.

Table 1. Adsorption energies of Gly on different vacancy defect concentrations of Mg(0001) surfaces.

Adsorption Energy	Vacancy Defect Concentrations			
	1/36	**1/6**	**1/3**	**1/2**
E_{ads} (eV)	−1.17	−1.26	−1.27; −1.40	−1.25; −1.15

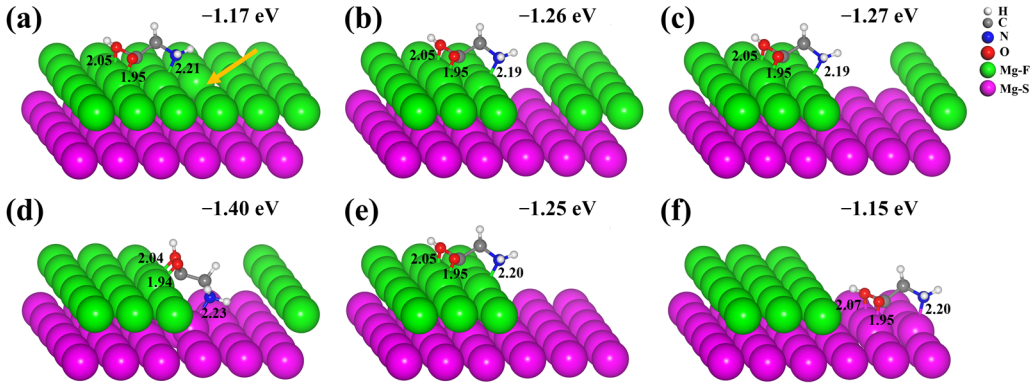

Figure 3. (**a**–**f**) are stable adsorption configurations of Gly on the Mg(0001) surfaces with the defect concentration of 1/36, 1/6, 1/3, 1/3, 1/2, and 1/2, respectively. Mg-F and Mg-S represent Mg atoms in the first and second layers, respectively.

The presence of defects has an impact on the electronic structure properties of the surface, which in turn affects the adsorption process of Gly. According to the calculated adsorption energy using Equation (1) in Table 1, it is observed that the presence of a single atomic vacancy defect on the Mg(0001) surface, as indicated by the arrow in Figure 3a,

results in an adsorption energy of −1.17 eV for Gly on this surface. In comparison to the adsorption energy of Gly on the defect-free Mg(0001) surface (−1.16 eV), the presence of a vacancy defect with a concentration of 1/36 slightly influences the adsorption energy of Gly, resulting in an adsorption energy of −1.17 eV. Figure 3b illustrates the optimized adsorption configuration of Gly on the Mg(0001) surface with a vacancy defect concentration of 1/6. In this configuration, the adsorption energy is −1.26 eV, indicating a higher stability compared to the adsorption on the Mg(0001) surface with a vacancy defect concentration of 1/36.

For the adsorption of Gly on the Mg(0001) surface with a defect concentration of 1/3, the optimized adsorption configurations are shown in Figure 3c,d. Considering the adsorption near and at the edge of the groove, the calculated E_{ads} are −1.27 eV and −1.40 eV, respectively. In comparison to the other cases shown in Figure 3, the configurations presented in Figure 3c,d exhibit higher E_{ads}. Among the six different adsorption configurations, the most stable configuration is observed when Gly is adsorbed at the edge of the groove. Considering defect surfaces with a vacancy defect concentration of 1/2, the adsorption of Gly near the edge and at the bottom of grooves was investigated. The optimized results for these adsorption configurations are depicted in Figure 3e,f, and the calculated E_{ads} are −1.25 and −1.15 eV, respectively. When Gly was adsorbed at the bottom of the vacancy defect groove, its adsorption energy was nearly equivalent to that on the surface of a defect-free Mg(0001) surface.

From the calculated results, the adsorption configuration of Gly at the edge of the grooved Mg(0001) surface with the vacancy defect is the most stable adsorption structure. The sharing of electrons from the adsorbent to the surface of Mg(0001) leads to a decrease in the length of the interaction bond to its optimal distance, resulting in an increase in the adsorption interaction energy. The optimized bond lengths of N1-Mg, O1-Mg, and O2-Mg in the adsorption systems shown in Figure 3 are approximately 2.19–2.23 Å, 1.94–1.95 Å, and 2.04–2.07 Å, respectively. These optimized bond lengths in Figure 3 are in close agreement with the sum of the covalent radii (2.11 and 2.09 Å) of nitrogen (0.75 Å) and oxygen (0.73 Å) atoms with the Mg (1.36 Å) atom, as reported in Ref. [47]. This agreement between the calculated bond lengths and the expected values is consistent with the results presented in Ref. [48].

3.2. Effect of Hydroxyl on the Adsorption of Gly on the Mg(0001) Surfaces

Under physiological conditions, the surfaces of Mg and Mg alloys are susceptible to hydroxylation, resulting in the formation of hydroxyl (hydroxide anion) on their surfaces. This hydroxyl presence has an impact on the binding properties of biomolecular coatings to these surfaces. To investigate the adsorption behavior of Gly on the Mg(0001) surface with hydroxyl, it is essential to determine the most stable position of the hydroxyl on the Mg(0001) surface. The optimized adsorption configurations of the hydroxyl at the four adsorption sites' (bridge, top, fcc-hollow, and hcp-hollow sites, as shown in Figure 1c) on the Mg(0001) surfaces are displayed in Figure 4. The calculated E_{ads} of the four adsorption cases by Equation (1) are depicted in Table 2.

Table 2. Adsorption energies of hydroxyl on the Mg(0001) surfaces.

Adsorption Energy	**Adsorption Site of Hydroxyl**			
	Bridge	**Top**	**Fcc-Hollow**	**Hcp-Hollow**
E_{ads} (eV)	−5.4581	−5.4569	−5.5010	−5.5004

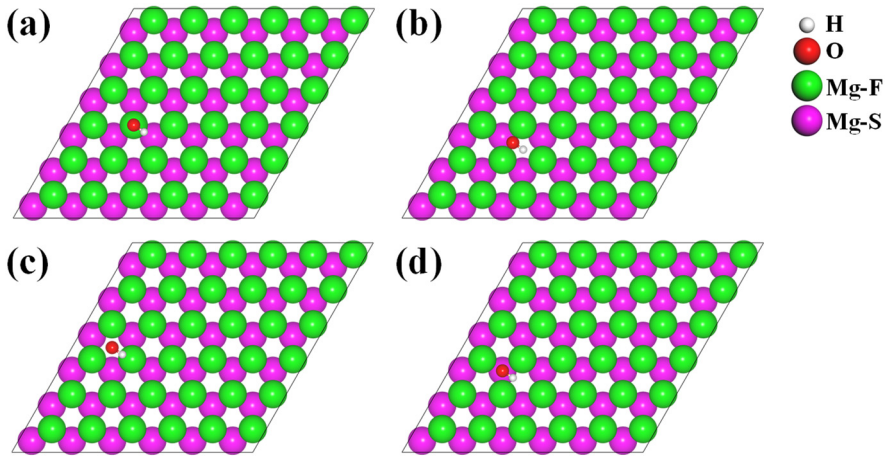

Figure 4. (**a**–**d**) correspond to the structures of hydroxyl adsorbed on the top, bridge, fcc, and hcp sites of Mg(0001) surface, respectively. The Mg-F and Mg-S labels indicate the Mg atoms in the first and second layers, respectively.

According to the optimized adsorption configurations of hydroxyl on the Mg(0001) surface in Figure 4 and the calculated E_{ads} by Equation (1) in Table 2, it can be seen that the E_{ads} of hydroxyl on the Mg(0001) surface for the four adsorption sites (bridge, top, fcc-hollow, and hcp-hollow sites) are −5.4581, −5.4569, −5.5010, and −5.5004 eV, respectively. The fcc-hollow site is the most favorable adsorption site among the four adsorption locations. Therefore, a Mg surface model with the hydroxyl adsorbed on the fcc-hollow site was selected as the surface for the adsorption of Gly. A hydroxylated Mg(0001) surface differs from the defect-free surface by the presence of a hydroxyl group (OH) that obtains some electrons from the surface. The optimized stable adsorption structure of Gly on the hydroxylated Mg(0001) surface, along with the selected bond lengths, is shown in Figure 5. The calculated E_{ads} of Gly on the Mg(0001) surface containing the hydroxyl is −1.11 eV, which is 0.05 eV more than the adsorption energy of Gly on the defect-free Mg(0001) surface (−1.16 eV) [32]. The presence of an additional OH group on the Mg(0001) surface leads to a slight decrease in the adsorption energy of Gly adsorption configurations. The sharing of electrons from the hydroxyl group to the Mg surface affects the overall binding energy between Gly and the Mg(0001) surface. This electron sharing leads to a decrease in the adsorption energy of Gly adsorption configurations.

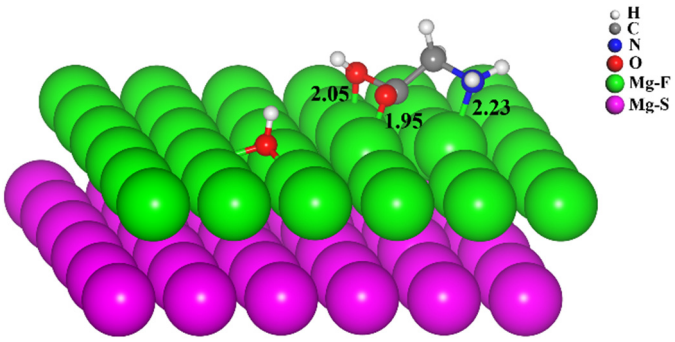

Figure 5. The optimized adsorption configuration of Gly on the hydroxylated Mg(0001) surface. The bond lengths (in Å) are also listed, and Mg-F and Mg-S represent Mg atoms in the first and second layers, respectively.

Based on the calculated results, it is observed that the adsorption of Gly on the hydroxylated Mg(0001) surface is accompanied by the release of a considerable amount of charge and energy. In the process of hydroxyl adsorption, some electrons are obtained from Mg atoms on the surface, resulting in corresponding changes in the electronic structure

properties of the surface. After stable adsorption, the interaction between the Mg(0001) surface containing hydroxyl and Gly is weakened. The bond lengths of O1-Mg, O2-Mg, and N-Mg are 1.95, 2.05, and 2.23 Å, respectively, which are close to the theoretical bond lengths for forming covalent bonds [47], and this result is also in good agreement with the results in Ref. [48].

3.3. Electronic Properties of Gly on Different Mg(0001) Surfaces

In this section, the interaction mechanism between orbitals during the formation of Gly and the defected/hydroxylated Mg(0001) surfaces was explored. As the results of previous sections suggest, the favorable adsorption structure of Gly at the edge of the groove in the defected adsorption system was focused. To analyze the electronic properties, the projected density of states (PDOS) of the Gly adsorption configurations on the mentioned substrates was examined. Specifically, the orbitals of the covalently bonded atoms before and after the adsorption were analyzed, as depicted in Figure 6.

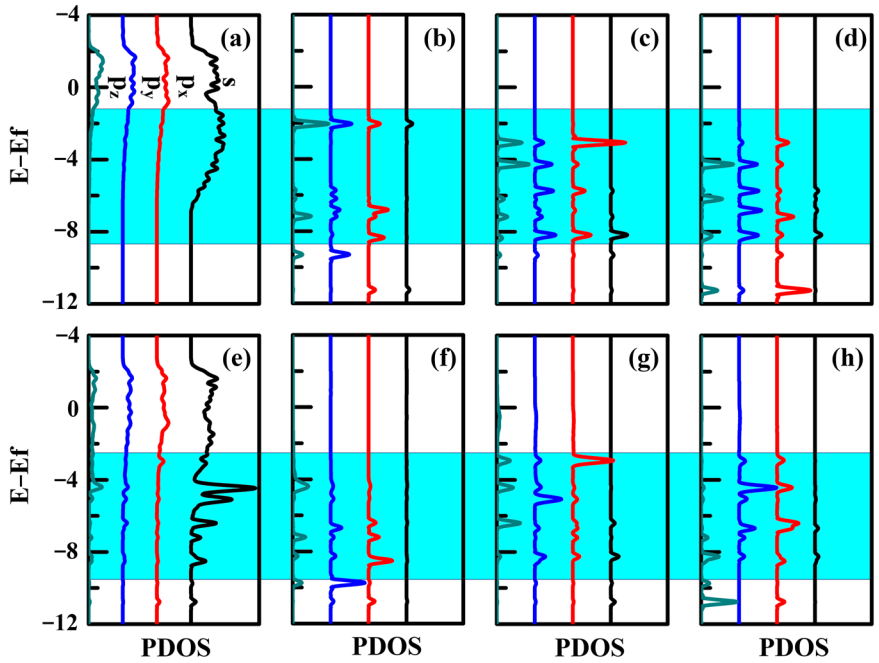

Figure 6. (**a**–**d**) are the PDOS of binding Mg atoms of the Mg(0001) surface, N1, O1, and O2 atoms of Gly before the adsorption; (**e**–**h**) are the PDOS of the corresponding atoms after adsorption, respectively. The Fermi level is set at 0 eV.

The calculated results in Figure 6 reveal that the electron localization of the binding atoms in isolated Gly decreases, and new peaks of the binding Mg atoms emerge after adsorption, in contrast to the results obtained before adsorption. A new peak overlap was observed between the N and Mg atoms at −4.30 eV in Figure 6e,f, which suggests the formation of a covalent bond between these atoms. This is evident from the shaded areas in the figure, where the PDOS curves of N and Mg atoms overlap, indicating the sharing of electrons and the formation of a chemical bond. The O1 atom that binds to the Mg atom on the surface exhibits overlapping peaks at −5.20 eV and −8.22 eV in Figure 6e,g. This indicates the formation of new covalent bonds between O1 and Mg. The shaded regions in the figure demonstrate this overlap, suggesting the sharing of electrons and the formation of chemical bonds between the O1 and Mg atoms. Indeed, it can be observed that the p-state electron localization of O1 is weakened after the surface adsorption of Gly, as compared to the results of Gly on the vacancy defect surface before adsorption. This can be seen in the PDOS curves of O1 in Figure 6g,h, where the peaks corresponding to the p-states of O1 become less pronounced after the adsorption of Gly on the Mg(0001) surface. This suggests a redistribution of electron density and a weakening of the electron

localization of O1 upon adsorption. Overlapping peaks of O2 and Mg atoms appear at the positions of −3.00 and −5.00 eV, indicating that O2 forms a new bond with surface Mg atoms, as depicted in the shaded areas in Figure 6e,h. According to the bond length values of each stable adsorption configuration in Figure 3, the bond lengths of N-Mg and O-Mg are close to the theoretical bond length of the covalent bond formed by them. The binding reason is mainly that the N in the amino group and the O in the carboxyl group share the lone pair electrons with the surface Mg atoms. Therefore, a coordination covalent bond is also formed between them when the defective Mg surface adsorbs Gly.

Further, the PDOS of Gly on the Mg(0001) surface with the hydroxyl adsorbed is plotted, as shown in Figure 4. This is an important process as hydroxylated Mg surfaces are very common on biomimetic coating surfaces.

One significant observation is the distinct downward displacement of the sp states of N and O in Figure 7. This indicates that the adsorption of Gly onto the hydroxylated Mg(0001) surface leads to a substantial reduction in electron localization within Gly. This considerable weakening of electron localization arises from the strong interaction that occurs between the N and O atoms of Gly and the surface. New peaks of N1-Mg atoms appear at the positions of −4.02, −6.21, and −8.10 eV in Figure 7e,f. At the same time, the O1 and Mg atoms exhibit new overlapping peaks at the positions of −3.80 and −4.10 eV, and the broadening range of O1 increases. This is mainly caused by the strong interaction between the *p*-orbital electrons of O1 and the s- and p-orbital electrons of the Mg surface atoms, as shown in the shaded regions in Figure 7e,g. The overlapping peaks of O2-Mg in Figure 7e,h appear at −3.80 and −4.20 eV, respectively.

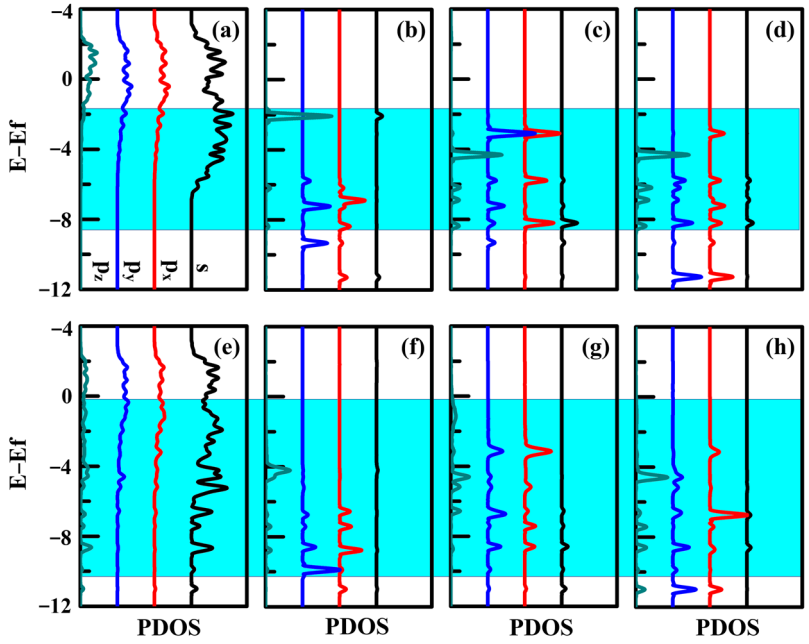

Figure 7. The PDOS of Gly on the hydroxylated Mg(0001) surface. (**a**–**d**) are the PDOS of Mg, N1, O1, and O2 atoms before adsorption, respectively; (**e**–**h**) are the PDOS of the corresponding atoms after adsorption, respectively.

The presence of overlapping peaks in the observed regions implies the formation of a novel chemical bond between Gly and the Mg surface atoms. The bonding process is mainly caused by the sharing of electrons between N and O atoms and Mg surface atoms. The bond lengths of N1-Mg, O1-Mg, and O2-Mg are close to the theoretical bond lengths for N/O and Mg to form a covalent bond. Therefore, Gly binds to the Mg surface containing defect/hydroxyl through coordinating covalent bonds.

4. Conclusions

In conclusion, the DFT calculations with the optb86b-vdw dispersion correction were utilized to investigate the impact of surface vacancy defects and hydroxyl on the adsorption characteristics of Gly on the Mg(0001) surface. All the possible adsorption configurations have been taken into account, and the interaction mechanism of Gly on different surface vacancy defect concentrations was also analyzed. Based on our analysis, the conclusions can be drawn as follows:

1. In the case of vacancy defects with varying concentrations, the most favorable adsorption mode of Gly on the Mg(0001) surface was found to involve the formation of coordination covalent bonds between the amino and carboxyl groups of Gly and the surface Mg atoms. Computational analysis revealed that the presence of defects facilitated a stronger adhesion of Gly to the surface compared to the defect-free surface. Specifically, the most stable configuration was observed when Gly was adsorbed at the edge of the grooved vacancy defect surface, with a defect concentration of 1/3.
2. Among the four adsorption sites, the fcc site is the most favorable adsorption site for the hydroxyl group. The adsorption of the hydroxyl group alters the electronic structure properties of the Mg(0001) surface, causing some electrons to transfer from the Mg(001) surface to the hydroxyl group, resulting in a slight decrease in the adsorption energy of Gly.
3. Different concentrations of vacancy defects can improve the adsorption of glycine on the Mg(0001) surface. The presence of the hydroxyl functional group weakens the adsorption of glycine on the Mg(0001) surface. These findings offer a theoretical foundation for the development of amino acid-based bio-coatings on material surfaces.

Author Contributions: Conceptualization, E.L.; Software, Y.J.; Writing—original draft, Z.F.; Writing—review & editing, S.G.; Visualization, H.Q.; Supervision, W.W. All authors have read and agreed to the published version of the manuscript.

Funding: The authors are very grateful for the financial support of the National Key Research and Development Program of China (2021YFC2400700), the Youth Fund Project of Zhongyuan University of Technology (K2022QN026), and the GHfund B 202302022245.

Institutional Review Board Statement: Not applicable.

Informed Consent Statement: Not applicable.

Data Availability Statement: Not applicable.

Conflicts of Interest: The authors declare no conflict of interest.

References

1. Kim, J.; Pan, H.B. Effects of magnesium alloy corrosion on biological response—Perspectives of metal-cell interaction. *Prog. Mater. Sci.* **2023**, *133*, 101039.
2. Farshid, S.; Kharaziha, M.; Atapour, M. A self-healing and bioactive coating based on duplex plasma electrolytic oxidation/polydopamine on AZ91 alloy for bone implants. *J. Magnes. Alloys* **2023**, *11*, 592–606.
3. Hou, R.Q.; Feyerabend, F.; Helmholz, H.; Garamus, V.M.; Willumeit-Roemer, R. Effects of proteins on magnesium degradation-static vs. dynamic conditions. *J. Magnes. Alloys* **2023**, *11*, 1332–1342.
4. Albaraghtheh, T.; Willumeit-Roemer, R.; Zeller-Plumhoff, B. In silico studies of magnesium-based implants: A review of the current stage and challenges. *J. Magnes. Alloys* **2022**, *10*, 2968–2996.
5. Kuah, K.X.; Wijesinghe, S.; Blackwood, D.J. Toward understanding in vivo corrosion: Influence of interfacial hydrogen gas build-up on degradation of magnesium alloy implants. *J. Biomed. Mater. Res. Part A* **2023**, *111*, 60–70. [CrossRef] [PubMed]
6. Mei, D.; Wang, C.; Lamaka, S.V.; Zheludkevich, M.L. Clarifying the influence of albumin on the initial stages of magnesium corrosion in Hank's balanced salt solution. *J. Magnes. Alloys* **2021**, *9*, 805–817.
7. Höhn, S.; Virtanen, S.; Boccaccini, A.R. Protein adsorption on magnesium and its alloys: A review. *Appl. Surf. Sci.* **2019**, *464*, 212–219.
8. Hou, R.Q.; Scharnagl, N.; Willumeit-Römer, R.; Feyerabend, F. Different effects of single protein vs. protein mixtures on magnesium degradation under cell culture conditions. *Acta Biomater.* **2019**, *98*, 256–268. [PubMed]

9. Cai, L.; Mei, D.; Zhang, Z.Q.; Huang, Y.D.; Cui, L.Y.; Guan, S.K.; Chen, D.C.; Kannan, M.B.; Zheng, Y.F.; Zeng, R.C. Advances in bioorganic molecules inspired degradation and surface modifications on Mg and its alloys. *J. Magnes. Alloys* **2022**, *10*, 670–688.
10. Hedberg, Y.S. Role of proteins in the degradation of relatively inert alloys in the human body. *npj Mater Degrad* **2018**, *2*, 1–5.
11. Rajan, S.T.; Arockiarajan, A. A comprehensive review of properties of the biocompatible thin films on biodegradable Mg alloys. *Biomed. Mater.* **2023**, *18*, 012002. [CrossRef]
12. Zhang, Z.Q.; Wang, H.Y.; Zeng, R.C. Protein conformation and electric attraction adsorption mechanisms on anodized magnesium alloy by molecular dynamics simulations. *J. Magnes. Alloys* **2022**, *10*, 3143–3155. [CrossRef]
13. Dai, J.H.; Xie, R.W.; Chen, Y.Y.; Song, Y. First principles study on stability and hydrogen adsorption properties of Mg/Ti interface. *Phys. Chem. Chem. Phys.* **2015**, *17*, 16594–16600. [CrossRef] [PubMed]
14. Savaedi, Z.; Motallebi, R.; Mirzadeh, H. A review of hot deformation behavior and constitutive models to predict flow stress of high-entropy alloys. *J. Alloys Compd.* **2022**, *903*, 163964. [CrossRef]
15. Li, Z.X.; Li, D.J.; Zhou, W.K.; Hu, B.; Zhao, X.F.; Wang, J.Y.; Qin, M.; Xu, J.K.; Zeng, X.Q. Characterization on the formation of porosity and tensile properties prediction in die casting Mg alloys. *J. Magnes. Alloys* **2022**, *10*, 1857–1867. [CrossRef]
16. Han, Z.Y.; Chen, H.P.; Zhou, S.X. Dissociation and diffusion of hydrogen on defect-free and vacancy defective Mg (0001) surfaces: A density functional theory study. *Appl. Surf. Sci.* **2017**, *394*, 371–377. [CrossRef]
17. Zhou, B.C.; Shang, S.L.; Wang, Y.; Liu, Z.K. Diffusion coefficients of alloying elements in dilute Mg alloys: A comprehensive first-principles study. *Acta Mater.* **2016**, *103*, 573–586. [CrossRef]
18. Williams, K.S.; Labukas, J.P.; Rodriguez-Santiago, V.; Andzelm, J.W. First Principles Modeling of Water Dissociation on Mg(0001) and Development of a Mg Surface Pourbaix Diagram. *Corrosion* **2014**, *71*, 209–223. [CrossRef]
19. Yuwono, J.A.; Birbilis, N.; Williams, K.S.; Medhekar, N.V. Electrochemical Stability of Magnesium Surfaces in an Aqueous Environment. *J. Phys. Chem. C* **2016**, *120*, 26922–26933. [CrossRef]
20. Zhou, W.L.; Liu, T.; Li, M.C.; Zhao, T.; Duan, Y.H. Adsorption of bromine on Mg(0001) surface from first-principles calculations. *Comput. Mater. Sci.* **2016**, *111*, 47–53. [CrossRef]
21. Li, B.X.; Xiao, C.C.; Harrison, N.M.; Fogarty, R.M.; Horsfield, A.P. Role of electron localisation in H adsorption and hydride formation in the Mg basal plane under aqueous corrosion: A first-principles study. *Phys. Chem. Chem. Phys.* **2023**, *25*, 5989–6001. [CrossRef]
22. Talha, M.; Ma, Y.C.; Kumar, P.; Lin, Y.H.; Singh, A. Role of protein adsorption in the bio corrosion of metallic implants—A review. *Colloids Surf. B Biointerfaces* **2019**, *176*, 494–506. [CrossRef]
23. Jackson, A.A. The Glycine story. *Eur. J. Clin. Nutr.* **1991**, *45*, 59–65.
24. Adeva-Andany, M.; Souto-Adeva, G.; Ameneiros-Rodriguez, E.; Fernandez-Fernandez, C.; Donapetry-Garcia, C.; Dominguez-Montero, A. Insulin resistance and glycine metabolism in humans. *Amino Acids* **2018**, *50*, 11–27. [CrossRef]
25. Yin, L.H.; Liu, X.P.; Yi, L.Y.; Wang, J.; Zhang, Y.J.; Feng, Y.F. Structural characterization of calcium glycinate, magnesium glycinate and zinc glycinate. *J. Innov. Opt. Health Sci.* **2016**, *10*, 1650052. [CrossRef]
26. Kanazawa, K.; Taninaka, A.; Takeuchi, O.; Shigekawa, H. What Orchestrates the Self-Assembly of Glycine Molecules on Cu(100)? *Phys. Rev. Lett.* **2007**, *99*, 216102. [CrossRef]
27. Pantaleone, S.; Rimola, A.; Ugliengo, P.; Sodupe, M. First-Principles Modeling of Protein/Surface Interactions. Polyglycine Secondary Structure Adsorption on the TiO_2 (101) Anatase Surface Adopting a Full Periodic Approach. *J. Chem. Inf. Model.* **2021**, *61*, 5484–5498. [CrossRef]
28. Xavier, N.F.; da Silva, A.M., Jr.; Sacchi, M.; Bauerfeldt, G.F. Decarboxylation of glycine on icy grain surfaces: A first-principle investigation. *Mon. Not. R. Astron. Soc.* **2022**, *517*, 5912–5920. [CrossRef]
29. Remko, M.; Rode, B.M. Effect of Metal Ions (Li^+, Na^+, K^+, Mg^{2+}, Ca^{2+}, Ni^{2+}, Cu^{2+}, and Zn^{2+}) and Water Coordination on the Structure of Glycine and Zwitterionic Glycine. *J. Phys. Chem. A* **2006**, *110*, 1960–1967. [CrossRef]
30. Zhu, C.; Wang, Q.; Huang, X.X.; Yun, J.N.; Hu, Q.L.; Yang, G. Adsorption of amino acids at clay surfaces and implication for biochemical reactions: Role and impact of surface charges. *Colloids Surf. B-Biointerfaces* **2019**, *183*, 110458. [CrossRef]
31. Madden, D.C.; Temprano, I.; Sacchi, M.; Jenkins, S.J. Spontaneous Local Symmetry Breaking: A Conformational Study of Glycine on Cu{311}. *J. Phys. Chem. C* **2015**, *119*, 13041–13049. [CrossRef]
32. Fang, Z.; Wang, J.F.; Yang, X.F.; Sun, Q.; Jia, Y.; Liu, H.R.; Xi, T.F.; Guan, S.K. Adsorption of arginine, glycine and aspartic acid on Mg and Mg-based alloy surfaces: A first-principles study. *Appl. Surf. Sci.* **2017**, *409*, 149–155. [CrossRef]
33. Fang, Z.; Wang, J.F.; Zhu, S.J.; Yang, X.F.; Jia, Y.; Sun, Q.; Jia, Y.; Guan, S.K. A DFT study of the adsorption of short peptides on Mg and Mg-based alloy surfaces. *Phys. Chem. Chem. Phys.* **2018**, *20*, 3602–3607. [CrossRef]
34. Fang, Z.; Zhao, Y.; Wang, H.Y.; Wang, J.F.; Zhu, S.J.; Jia, Y.; Cho, J.Y.; Guan, S.K. Influence of surface charge density on ligand-metal bonding: A DFT study of NH3 and HCOOH on Mg (0001) surface. *Appl. Surf. Sci.* **2019**, *470*, 893–898. [CrossRef]
35. Fang, Z.; Ding, H.L.; Li, P.; Qiao, H.J.; Liang, E.J.; Jia, Y.; Guan, S.K. Interaction Mechanism of RGD Tripeptide on Different Surfaces of Mg and Mg Alloys: A First-Principles Study. *Coatings* **2022**, *12*, 1814. [CrossRef]
36. Kresse, G.; Furthmüller, J. Efficient iterative schemes for ab initio total-energy calculations using a plane-wave basis set. *Phys. Rev. B* **1996**, *54*, 11169–11186. [CrossRef]
37. Kresse, G.; Furthmüller, J. Efficiency of ab-initio total energy calculations for metals and semiconductors using a plane-wave basis set. *Comput. Mater. Sci.* **1996**, *6*, 15–50. [CrossRef]
38. Blöchl, P.E. Projector augmented-wave method. *Phys. Rev. B* **1994**, *50*, 17953–17979. [CrossRef]

39. Perdew, J.P.; Burke, K.; Ernzerhof, M. Generalized Gradient Approximation Made Simple. *Phys. Rev. Lett.* **1996**, *77*, 3865–3868. [CrossRef]
40. Dion, M.; Rydberg, H.; Schröder, E.; Langreth, D.C.; Lundqvist, B.I. Van der Waals Density Functional for General Geometries. *Phys. Rev. Lett.* **2004**, *92*, 246401. [CrossRef]
41. Klimeš, J.; Bowler, D.R.; Michaelides, A. Chemical accuracy for the van der Waals density functional. *J. Phys. Condens. Matter* **2010**, *22*, 022201. [CrossRef]
42. Klimeš, J.; Michaelides, A. Perspective: Advances and challenges in treating van der Waals dispersion forces in density functional theory. *J. Chem. Phys.* **2012**, *137*, 120901. [CrossRef]
43. Klimeš, J.; Bowler, D.R.; Michaelides, A. Van der Waals density functionals applied to solids. *Phys. Rev. B* **2011**, *83*, 195131. [CrossRef]
44. Lüder, J.; Sanyal, B.; Eriksson, O.; Puglia, C.; Brena, B. Comparison of van der Waals corrected and sparse-matter density functionals for the metal-free phthalocyanine/gold interface. *Phys. Rev. B* **2014**, *89*, 045416. [CrossRef]
45. Swanson, H.E.; McMurdie, H.F.; Morris, M.C.; Evans, E.H. Standard X-ray Diffraction Powder Patterns. In *National Bureau of Standards Monograph 25—Section 6*; U.S. Department of Commerce, National Bureau of Standards: Gaithersburg, MD, USA, 1968.
46. Lei, H.P.; Wang, C.Z.; Yao, Y.X.; Wang, Y.G.; Hupalo, M.; McDougall, D.; Tringides, M.; Ho, K.M. Strain effect on the adsorption, diffusion, and molecular dissociation of hydrogen on Mg (0001) surface. *J. Chem. Phys.* **2013**, *139*, 224702. [CrossRef]
47. Sargent, W. *Table of Periodic Properties of the Elements*; Sargent-Welch Scientific: Skokie, IL, USA, 1980.
48. Hoffling, B.; Ortmann, F.; Hannewald, K.; Bechstedt, F. Single cysteine adsorption on Au(110): A first-principles study. *Phys. Rev. B* **2010**, *81*, 045407. [CrossRef]